THE ASTROPHYSICAL JOURNAL, 412:173–182, 1993 July 20

OXYGEN ABUNDANCES IN F-TYPE STARS OF THE HYADES AND THE URSA MAJOR GROUP[1]

RAMÓN J. GARCÍA LÓPEZ, RAFAEL REBOLO, ARTEMIO HERRERO, AND JOHN E. BECKMAN
Instituto de Astrofísica de Canarias, E-38200, La Laguna, Tenerife, Spain
Received 1992 July 31; accepted 1993 January 15

ABSTRACT

We have derived the oxygen abundances of 50 F-type main-sequence stars, belonging to the Hyades open cluster, the Ursa Major group, and the field, using an NLTE analysis of the infrared triplet lines of O I at $\lambda\lambda$7771–7775. The stars of the middle F-range ($6500 < T_{\rm eff} < 6900$ K) have previously been shown to exhibit a marked reduction in lithium abundance compared with both cooler and hotter objects in the same systems: the "Li gap," for which several explanations have been proposed. Our results here show a substantial measure of uniformity in the oxygen abundances over the range in $T_{\rm eff}$ between 5800 and 7400 K. The data might indicate a small dip (<0.1 dex) in the oxygen abundance for stars located in the Li gap. Microscopic diffusion seems to be the only known mechanism able to produce an oxygen dip. If this mechanism were also responsible for the Li gap, it would have to account for a depletion of up to two orders of magnitude in lithium and, at the same time, less than 0.1 dex in oxygen. We note, however, that turbulent mixing could modify a microscopic diffusion pattern in order to yield the observed abundances. Our oxygen abundances for the Hyades and the Ursa Major group stars fit well a trend of increasing [O/H] ratio with increasing metallicity, as observed in the Galactic disk for stars in the range $-0.8 \leq$ [Fe/H] $\leq +0.3$. There is, however, a strong scatter in this trend for stars with [Fe/H] > 0. On the other hand, the [O/H] cluster values imply an evolution of [O/H] with age which is flatter than that inferred for field stars only.

Subject headings: open clusters and associations: individual (Hyades, Ursa Major) — stars: abundances

1. INTRODUCTION

Clusters and associations present us with opportunities to analyze with considerable precision the chemical composition of homogeneous samples of stars whose physical parameters can be well determined, thus reducing the uncertainty inherent in abundance determination of isolated field stars. In F-type stars of the Hyades and Ursa Major group, the abundance of lithium has been measured in many objects by Boesgaard and her coworkers (Boesgaard & Tripicco 1986a; Boesgaard 1987a; Boesgaard, Budge, & Burck 1988; Boesgaard & Budge 1988), who found a strong dip in the lithium abundance in both groups of stars, in the effective temperature range 6400–6900 K. This "Li gap" has also been observed in other clusters and associations—NGC 752 (Hobbs & Pilachowski 1986, 1988; Beckman & Rebolo 1988), Coma (Boesgaard 1987b), Praesepe (Boesgaard & Budge 1988), NGC 6475 (Balachandran 1991), and field stars (Boesgaard & Tripicco 1986b, 1987; Balachandran 1990a; Lambert, Heath, & Edvardsson 1991)—and is a phenomenon of considerable value for studying the structure and evolution of F stars. To account for the gap, several transport mechanisms have been proposed to explain the Li depletion. These mechanisms can be divided into two different groups: those which invoke the nuclear burning of the Li atoms and those in which this is not necessary. The latter group contains the microscopic diffusion (Michaud 1986) and superficial mass-loss models (Schramm, Steigman, & Dearborn 1990), while the former group includes meridional circulation (Charbonneau & Michaud 1988), rotationally induced turbulent mixing (Vauclair 1988; Charbonnel, Vauclair, & Zahn 1992), mixing induced by internal braking, that is, by radial angular momentum transport (Pinsonneault, Kawaler, & Demarque 1990), and mixing induced by internal gravity waves (García López & Spruit 1991).

The mechanism of microscopic diffusion operates where the material sinks below the surface convection zone because the internal radiation pressure is not capable of supporting the weight of the nuclide concerned. Extrapolating from previous calculations for helium, Michaud (1988) suggested that if the outward radiative acceleration is insufficient to support Li in the outer layers of an F star against the inward acceleration due to gravity, the same could then hold for nitrogen and oxygen. Thus if the observed Li depletion in the F stars were due to microscopic diffusion, we could expect to find similar effects for these other elements, which would not be predicted for the other mechanisms quoted above.

With this test in mind, we set about measuring the oxygen abundance in the F stars of the Hyades (age ~ 6–8×10^8 yr) and of Ursa Major group (age $\sim 3 \times 10^8$ yr), and also of a group of evolved stars whose age is estimated to be around 10^9 yr. In almost all these stars there were already measurements of the Li abundances and [Fe/H], where $[X/{\rm H}] = \log (X/{\rm H})_{\rm star} - \log (X/{\rm H})_{\odot}$, in the literature. The use of the metallicities has also allowed us to study the average ratio [O/H] in both open clusters and its relation to a general trend [O/H] versus [Fe/H] derived from measurements in field stars with $-0.8 \leq$ [Fe/H] $\leq +0.3$ by Nissen & Edvardsson (1992).

We selected the permitted triplet of oxygen I comprising the three lines at $\lambda\lambda$7771.944, 7774.167, and 7775.388, which are produced by the transition between the metastable $3s\ ^5S^0_2$ level and the $3p\ ^5P_{3,2,1}$ level. This triplet is easily observable in stars in the range of spectral types between B and late G. The sensitivity of the line to non-LTE effects is well known and studied (Sedlmayr 1974; Baschek, Scholz, & Sedlmayr 1977; Eriksson & Toft 1979; Sneden, Lambert, & Whitaker 1979; Faraggiana

[1] Based on observations made with the Isaac Newton Telescope, operated on the island of La Palma by the Royal Greenwich Observatory in the Spanish Observatorio del Roque de los Muchachos of the Instituto de Astrofísica de Canarias; and with the 2.2 m telescope of the German-Spanish Observatorio de Calar Alto, Almería, Spain.

et al. 1988; Abia & Rebolo 1989; Kiselman 1991; Bessell, Sutherland, & Ruan 1991). In the present study we carried out a non-LTE analysis which confirms the significant differences between the abundances derived using LTE and NLTE, and the need to take carefully these into account.

2. OBSERVATIONS AND DATA REDUCTION

The observations were performed during a series of observing runs on the 2.5 m Isaac Newton Telescope of the Observatorio del Roque de los Muchachos (La Palma) and the 2.2 m telescope of the Observatorio de Calar Alto (Almería). The first of these runs took place on 1989 October 25 and 26 on the 2.2 m telescope at Calar Alto. We used the Boller and Chivens spectrograph at the coudé focus, at f/12 focal ratio, and with the no. 1 grating (632 line mm^{-1}) in first order, at grating angle 17°55'.2 which corresponds to a central wavelength of λ7782.3 and yields a dispersion of 4.4 Å mm^{-1}. To eliminate light from other orders we introduced an OG615 color filter, which passed light only longwards of 6150 Å. We used an RCA CCD camera of 360 × 1024 pixels each of dimension 15 μm × 15 μm. To achieve a satisfactory compromise between resolution and illumination we observed with a 200 μm slit which subtended an angle of ~0".5 on the sky. The projection of this slit on the detector was 58 μm. To reduce the effective readout noise we decided to combine detector pixels in two's in the spectral direction and in three's in the spatial direction. The final slit-limited spectral resolution was 0.255 Å ($\lambda/\Delta\lambda \sim 3 \times 10^4$), adequate for the purpose of resolving the triplet lines, at least in those stars of our sample with low $v \sin i$.

The remaining observations of the O I triplet were carried out during the nights 1990 March 13–15, and on 1991 January 1, 2, and 20–24 using the Isaac Newton Telescope. We used the intermediate dispersion spectrograph (IDS) and a GEC CCD detector (400 × 590 pixels with pixel size 22 μm × 22 μm) in the 500 mm camera. The grating (H1800V) which had 1800 lines mm^{-1} was used in first order giving a dispersion of 9.8 Å mm^{-1}. During these observing runs the spectrograph entrance slit aperture was varied between 150 and 180 μm, depending on the seeing, corresponding to an angle on the sky of between 0".8 and 1". The slit width projected onto the detector was between 36 and 44 μm, giving a spectral resolution in the range 0.353–0.431 Å ($\lambda/\Delta\lambda \sim 1.8$–$2.2 \times 10^4$). Table 1 shows the stars observed, giving their visual magnitudes, rotational velocities ($v \sin i$), observation dates, and exposure times.

TABLE 1

STARS OBSERVED

Star	V	$v \sin i$ (km s^{-1})	obs.	exp. t. (s)
HYADES				
VB6	5.97	50	1	2400
VB8	6.37	50	1	3000
VB11	6.01	25	2	300
VB13	6.62	18	2	500
VB14	5.73	≤ 12	2	300
VB19	7.14	≤ 12	1	3600
VB20	6.32	55	1	3600
VB31	7.47	10	2	1000
			4	2000
VB35	6.80	90	4	1000
VB37	6.61	12	2	500
VB38	5.72	15	2	300
VB44	7.19	30	2	800
			4	500
VB48	7.14	≤ 12	4	600
VB61	7.38	18	2	900
VB65	7.42	9	2	1000
			4	1000
VB66	7.51	–	4	1000
VB78	6.92	20	2	800
VB81	7.10	18	4	300
VB85	6.51	55	1	3600
VB86	7.05	20	2	800
VB88	7.78	–	4	1200
VB90	6.40	35	2	500
VB94	6.62	40	2	500
VB100	6.02	80	4	500
VB101	6.65	40	1	3000
VB105	7.53	–	4	1000

Star	V	$v \sin i$ (km s^{-1})	obs.	exp. t. (s)
URSA MAJOR				
HR235	5.19	3.5	1	1800
HR330	5.52	–	1	1800
HR534	5.94	–	1	1800
HR647	6.06	< 26	4	600
HR1983	3.60	11	4	120
HR2047	4.41	9.4	1	1000
HR3064	5.17	< 17	3	400
			4	1300
HR3391	5.64	9.5	3	300
HR4150	6.28	8	3	300
HR4867	5.85	36	4	250
HR5328	6.69	40	3	800
HR5365	5.41	39	3	250
HR5634	4.93	45	3	200
HR5830	5.75	–	3	350
			4	300
HR7061	4.19	14	1	2800
			4	100
HR7312	5.13	63	1	1800
HR7451	5.73	6.5	1	1800
HD151044	6.64	5.4	4	250
FIELD				
HR5011	5.22	7	4	180
HR5235	2.68	11	4	50
HR5363	6.32	31	4	300
HR5445	6.33	15	4	300
HR5529	6.16	15	4	300
HR5612	6.65	18	4	300

NOTES.—The visual magnitudes of the Hyades stars were taken from Mermilliod 1976 and their rotation velocities from Kraft 1965. For the stars in the Ursa Major group, visual magnitude V and $v \sin i$ come from the Bright Star Catalogue (Hoffleit & Jaschek 1982). For the field stars, the visual magnitudes were taken from this catalog, while the $v \sin i$ values come from Balachandran 1990a. In col. (4) the observation data are coded as follows: (1) 1989 October 25–26, (2) 1990 March 13–15, (3) 1991 January 1–2, (4) 1991 January 20–24.

All the observations were reduced using the IRAF suite of programs.[2] The procedure was the following: bias subtraction, flat-field division, extraction of one-dimensional spectrum, and continuum normalization. Where we had more than one spectrum of a single object, these were co-added, displacing them if necessary to bring them into wavelength registration. The continuum normalization took place after we had produced a single one-dimensional spectrum for each object. As these stellar spectra include a number of photospheric lines, we were able to calibrate in wavelength using the slow rotators (small $v \sin i$, sharp lines) observed in any given observing series. The photospheric wavelengths were taken from the solar atlas of Moore, Minnaert, & Houtgast (1966). A second-order polynomial was used, on the basis of 8–10 spectral lines, to give calibrations with rms scatter between 0.004 and 0.007 Å, showing that the dispersions were 0.130 and 0.200 Å pixel^{-1}, respectively, for the Calar Alto and La Palma observations.

Figure 1 shows two examples of the reduced spectra: VB31, a cool slow rotator, and VB94, an intermediate F-type star with high-rotation velocity. The signal-to-noise ratios in the Calar Alto spectra were between 70 and 170, while for La Palma spectra the S/N was close to 150 in all cases. In Table 2 we give the measured equivalent widths for the stars of our samples. These equivalent widths were obtained by integrating over the triplet as a whole, and not over each line separately, because the sample contains a number of rapid rotators whose triplet lines are blended. The procedure adopted guaranteed uniformity between these stars and the slow rotators with unblended lines. In order to see if there are any differences in the oxygen abundances derived from the whole triplet and from each of the three lines, we also measured separately their individual equivalent widths in 12 stars with unblended lines covering the effective temperature range of the whole sample. As we will see in § 3, there are no differences between the mean abundance value provided by the three lines separately in a given star and that obtained using the integrated triplet. The uncertainty in an equivalent width estimate was due largely to the difficulty in placing the continuum level in a given spectrum. As seen in Figure 2, there is a clear increase in equivalent width with effective stellar temperature due to the increasing population of higher O I levels at higher temperatures, enhanced somewhat by non-LTE effects, which also increase with increasing temperature.

[2] IRAF is distributed by National Optical Astronomy Observatories, which is operated by the Association of Universities for Research in Astronomy, Inc., under contract with the National Science Foundation.

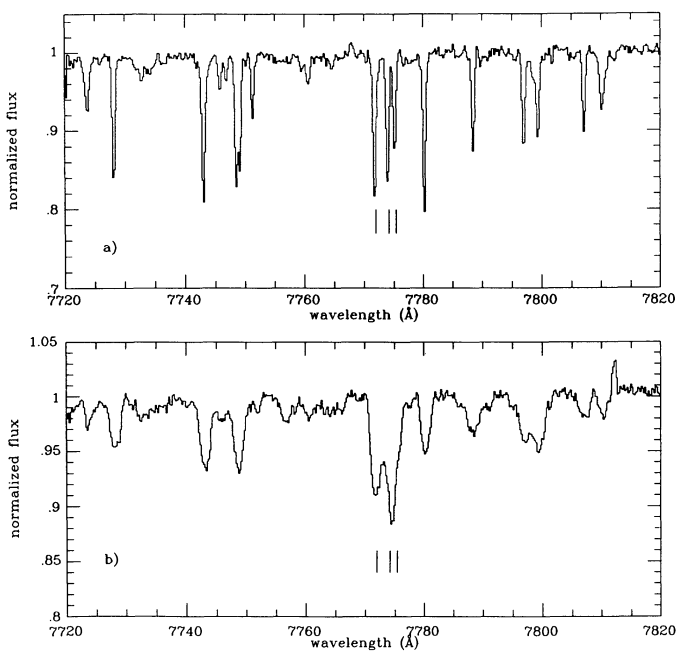

FIG. 1.—Two examples of the spectra obtained for the O I IR triplet from the stars treated in this study. (*a*) VB31 ($T_{\rm eff}$ = 6045 K and $v \sin i$ = 10 km s^{-1}); (*b*) VB94 ($T_{\rm eff}$ = 6650 K and $v \sin i$ = 40 km s^{-1}).

3. DATA ANALYSIS

3.1. *The Model of the Oxygen Atom*

The oxygen triplet was analyzed in NLTE using the model atom of Baschek et al. (1977), in which only the fundamental state, seven excited states, and the continuum are considered. These authors justify the use of this restricted number of levels due to the low population of levels with energies higher than that of the $4d\ ^5D^o$ level, and the fact that these upper levels are collisionally coupled to the continuum. Furthermore, other transitions between the levels considered, such as the forbidden λ6726 line between the $3s\ ^5S^o$ and $3p\ ^3P$ levels, are very weak compared with the transitions taken into account. All transitions involving the ground level of O I were set in detailed balance (i.e., $n_1 R_{1j} = n_j R_{j1}$, where n_i is the population of the ith level, and R_{ij} is the radiative transition rate from level i to level j). This is justified by the fact that the first excited level of O I lies well above the ground level (ΔE = 9.145 eV), so at the temperatures of our stars the latter is many orders of magnitude more populated than any other O level, and thus all its transitions are optically thick. Finally only the ground state of O II has been considered, due to the high-ionization potential of O I.

The values of the oscillator strengths, f, for each transition were taken from Wiese, Smith, & Glennon (1966). Biémont et al. (1991) present new calculations of oscillator strengths for a set of transitions due to neutral oxygen. Their calculations, using two different theoretical treatments (Hibbert 1975 and

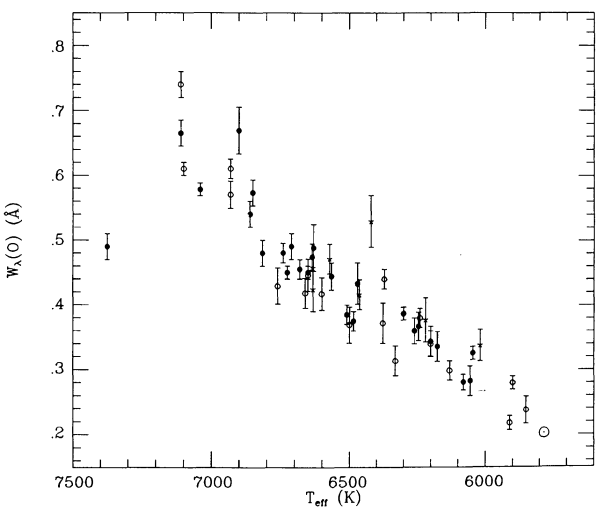

FIG. 2.—Equivalent width of the O I IR triplet vs. $T_{\rm eff}$ for all the stars measured here. *Filled circles*: Hyades; *open circles*: Ursa Major group; asterisks: field stars.

TABLE 2

OXYGEN EQUIVALENT WIDTHS AND ABUNDANCES

Star	T_{eff} (K)	W_λ(O) (Å)	log N(O) LTE	log N(O) NLTE	[O/H]
HYADES					
VB38	7375	0.490±0.020	9.20	8.79±0.13	−0.37 ± 0.13
VB6	7110	0.665±0.020	9.97	9.42±0.13	+0.26 ± 0.13
VB14	7040	0.578±0.010	9.68	9.18±0.13	+0.02 ± 0.13
VB100	6900	0.669±0.035	10.11	9.53±0.17	+0.37 ± 0.17
VB20	6860	0.540±0.020	9.65	9.16±0.14	+0.00 ± 0.14
VB11	6850	0.573±0.020	9.78	9.27±0.14	+0.11 ± 0.14
VB37	6815	0.480±0.020	9.44	9.02±0.15	−0.14 ± 0.15
VB90	6740	0.480±0.015	9.49	9.07±0.14	−0.09 ± 0.14
VB13	6725	0.450±0.010	9.39	8.98±0.14	−0.18 ± 0.14
VB8	6710	0.490±0.020	9.56	9.11±0.15	−0.05 ± 0.15
VB85	6680	0.455±0.015	9.44	9.03±0.15	−0.13 ± 0.15
VB94	6650	0.450±0.010	9.44	9.04±0.15	−0.12 ± 0.15
VB101	6635	0.474±0.020	9.55	9.11±0.15	−0.05 ± 0.15
VB35	6630	0.488±0.035	9.61	9.16±0.18	+0.00 ± 0.18
VB44	6565	0.444±0.020	9.49	9.08±0.15	−0.08 ± 0.15
VB78	6510	0.385±0.015	9.29	8.93±0.16	−0.23 ± 0.16
VB86	6485	0.375±0.015	9.27	8.92±0.16	−0.24 ± 0.16
VB81	6470	0.433±0.030	9.52	9.12±0.17	−0.04 ± 0.17
VB19	6300	0.387±0.010	9.50	9.12±0.17	−0.04 ± 0.17
VB61	6260	0.360±0.020	9.42	9.08±0.18	−0.08 ± 0.18
VB48	6245	0.367±0.020	9.47	9.11±0.16	−0.05 ± 0.16
VB65	6200	0.344±0.020	9.42	9.09±0.16	−0.07 ± 0.16
VB88	6175	0.336±0.020	9.41	9.09±0.16	−0.07 ± 0.16
VB66	6080	0.281±0.010	9.26	9.00±0.17	−0.16 ± 0.17
VB105	6055	0.283±0.020	9.30	9.04±0.19	−0.12 ± 0.19
VB31	6045	0.326±0.010	9.53	9.20±0.18	+0.04 ± 0.18
URSA MAJOR					
HR7312	7110	0.740±0.020	10.26	9.64±0.13	+0.48 ± 0.13
HR534	7100	0.610±0.010	9.77	9.25±0.12	+0.09 ± 0.12
HR330	6930	0.610±0.015	9.87	9.36±0.14	+0.20 ± 0.14
HR5830	6930	0.570±0.020	9.72	9.23±0.14	+0.07 ± 0.14
HR5328	6760	0.429±0.030	9.28	8.83±0.17	−0.27 ± 0.17
HR4150	6660	0.418±0.020	9.30	8.92±0.16	−0.24 ± 0.16
HR5365	6650	0.446±0.025	9.42	9.02±0.16	−0.14 ± 0.16
HR5634	6600	0.417±0.025	9.34	8.96±0.16	−0.20 ± 0.16
HR647	6500	0.369±0.030	9.23	8.88±0.18	−0.28 ± 0.18
HR4867	6376	0.372±0.030	9.34	9.01±0.18	−0.15 ± 0.18
HR7061	6370	0.440±0.015	9.65	9.22±0.15	+0.06 ± 0.15
HR1983	6329	0.314±0.020	9.16	8.84±0.17	−0.32 ± 0.17
HR7451	6240	0.380±0.015	9.54	9.16±0.18	+0.00 ± 0.18
HR235	6200	0.340±0.020	9.40	9.07±0.18	−0.09 ± 0.18
HD151044	6130	0.299±0.015	9.29	9.01±0.18	−0.15 ± 0.18
HR3064	5910	0.218±0.010	9.18	8.98±0.20	−0.18 ± 0.20
HR2047	5900	0.280±0.010	9.51	9.23±0.19	+0.07 ± 0.19
HR3391	5850	0.238±0.020	9.37	9.14±0.20	−0.02 ± 0.20
FIELD					
HR5529	6632	0.424±0.035	9.34	8.96±0.17	−0.20 ± 0.17
HR5612	6572	0.471±0.020	9.59	9.15±0.16	−0.01 ± 0.16
HR5445	6463	0.416±0.020	9.46	9.07±0.16	−0.09 ± 0.16
HR5363	6420	0.529±0.040	9.98	9.46±0.20	+0.30 ± 0.20
HR5235	6219	0.377±0.035	9.55	9.17±0.18	+0.01 ± 0.18
HR5011	6018	0.338±0.025	9.62	9.27±0.20	+0.11 ± 0.20

Cowan 1981) yield log g_f values similar to those we used for the O I triplet lines: 0.35 and 0.4 compared to 0.333, 0.21 and 0.25 compared to 0.186, and −0.02 and −0.03 compared with −0.035.

3.2. *The Spectral Synthesis Code*

Our spectral synthesis was performed using the code described by Giddings (1981; see Butler & Giddings 1985). This code solves the coupled equations of statistical equilibrium and radiative transport for a generalized atom using complete linearization with the formalism put forward by Auer & Heasley (1976). In the computation of the theoretical profiles we took account of the effect of radiative damping using the expression for the damping coefficient $\gamma_{\rm rad}$,

$$\gamma_{\rm rad} = 6.66 \times 10^{15} \frac{g_l}{g_u} \frac{f}{\lambda^2} (\mathrm{s}^{-1}) , \quad (1)$$

with λ expressed in Å, and where f is the oscillator strength and g_u and g_l the statistical weights, respectively, of the upper and lower transition levels (given in Table 1 of Baschek et al. 1977). We also took into account van der Waals broadening, using Gray's (1976) form of Unsöld's (1955) approximation for the damping constant $\gamma_{\rm vdW}$:

$$\log \gamma_{\rm vdW} \cong 19.6 + \tfrac{2}{5} \log C_6 + \log P_g - \tfrac{7}{10} \log T , \quad (2)$$

where T is the temperature in kelvins, P_g the gas pressure in cgs, and

$$C_6 = 1.872 \times 10^{-30} Z^2 [(\chi_I - \chi_u)^{-2} - (\chi_I - \chi_l)^{-2}] , \quad (3)$$

where Z takes the value 1 for a neutral atom, 2 for a singly ionized atom, etc., χ_I is the ionization potential, in eV, and χ_l and χ_u are the excitation potentials of the lower and upper transition levels, respectively, also in eV. We also included the quadratic Stark effect, following the expression given by Gray (1976) for the Stark broadening coefficient $\gamma_{\rm Stark}$:

$$\log \gamma_{\rm Stark} \cong 19.4 + \tfrac{2}{3} \log C_4 + \log P_e - \tfrac{5}{6} \log T , \quad (4)$$

where P_e is the electron pressure, in cgs, and C_4 is the interaction constant. This broadening term was only needed for the λ7773 triplet transitions themselves; for the other transitions the Doppler broadening was enough. For the O I triplet we wanted to obtain precise information about the lines, while we were interested only in the level populations for the remaining transitions. The values taken for C_4 and C_6 from Baschek et al. (1977) were $\log C_4 = -14.46$ and $\log C_6 = -30.87$. In fact this value for C_6 is one-third of that obtained directly from the Unsöld (1955) approximation (eq. [3]). It is common practice to multiply the constant C_6 derived from equation (3) by a normalizing factor so that the synthetic profiles fit the observed profiles (see, e.g., Gray 1976 and references therein). As we will see below, this arbitrary normalization yields an uncertainty in the absolute values of the derived abundances.

The ionization and free-free absorption cross sections were taken from Hofsaess (1979) while the collisional transition were calculated using the approximation due to Seaton (1962) and van Regemorter (1962). The spectral synthesis made use of the model atmospheres of Kurucz (1979).

3.3. *Choice of Stellar Parameters*

Almost all of the stars we have selected here for oxygen abundance determination had been previously studied to derive their lithium abundances, and we were able to use effective temperature determinations by the authors of the papers concerned: Boesgaard & Tripicco (1986a) for the Hyades, Boesgaard et al. (1988) for the Ursa Major group, and Balachandran (1990a) for field stars. To obtain an adequate sample in the $T_{\rm eff}$ range of the Li gap we observed three additional Hyades stars and two in the Ursa Major group for which there were no previous lithium measurements. For these stars we calculated the effective temperature using the mean given by the three equations of the semiempirical calibration for F stars of Saxner & Hammarbäck (1985), in terms of Johnson, Strömgren, and Hβ photometry and metallicity (these three expressions were used by Boesgaard et al. 1988 for the Ursa Major group), and using the calibration adopted by Boesgaard & Tripicco (1986a) and Boesgaard & Budge (1988) for the Hyades. The typical uncertainty in one of these temperatures is ± 100 K. The photometric data for these five stars were taken from Crawford & Perry (1966) for the Hyades, and Hauck & Mermilliod (1980) for the Ursa Major group, and were not corrected for interstellar extinction because of the proximity of these clusters. The [Fe/H] values used in the calibration of Saxner & Hammarbäck (1985) were +0.12 for the Hyades (Cayrel, Cayrel de Strobel, & Campbell 1985) and −0.08 for the Ursa Major group (Boesgaard et al. 1988). Using the method described we analyzed a total of 50 stars, 26 from the Hyades, 18 from the Ursa Major group, and six field stars, with effective temperatures in the range 5850–7375 K. The complete list of stars, ordered by decreasing $T_{\rm eff}$, is given in Table 2.

The log g values were estimated following the procedure indicated by Boesgaard & Trippico (1986b), using values of Strömgren photometry from Crawford & Perry (1966) and Hauck & Mermilliod (1980). The mean value for all the stars was log $g = 4.18 \pm 0.08$, in a range encompassing 3.9–4.4. We have not needed to list individual log g values here, because the interpolative procedure for determining abundances in individual stars was performed only against $T_{\rm eff}$ as variable, given the moderate dependence on log g and its relatively small variation within the sample. However, as we see below, a series of models was produced with incremental variations of 0.3 dex in log g to estimate the error in the abundance which would correspond to a variation of this amplitude.

In the light of the steller parameters derived for the sample stars, we generated the grid of models outlined in Table 3. The first seven models cover the effective temperature range of our stars. In all of these we adopted a value of 4.2 for log g: an average, but quite adequate as explained above. For each $T_{\rm eff}$ and log g we used the microturbulence parameter for F stars from the expression by Nissen (1981). The remaining models were used to estimate uncertainties corresponding to variations in the stellar parameters. Finally we used a model with parameters appropriate to the solar atmosphere ($T_{\rm eff} = 5770$ K, log $g = 4.44$, and $\xi = 1.1$ km s^{-1}) in order to compare the F-star oxygen abundances directly with that of the Sun, adopting an identical analytical procedure.

TABLE 3

GRID OF MODELS GENERATED

No.	$T_{\rm eff}$ (K)	log g (cm s^{-2})	ξ (km s^{-1})
1	5900	4.20	1.49
2	6000	4.20	1.52
3	6250	4.20	1.60
4	6500	4.20	1.68
5	6750	4.20	1.76
6	7000	4.20	1.84
7	7375	4.20	1.96
8	6500	4.50	1.68
9	6500	4.20	1.90
10	6500	4.50	1.29
11	7000	4.00	1.84

3.4. *Derivation of the Abundances*

Due to the fact that the NLTE calculations imply a considerable amount of computing time, we decided to produce a suitable grid of theoretical profiles including each line of the triplet. For each of the first seven models of Table 3 we produced three different synthetic profiles using the three oxygen abundances log N(O) = 9.34, 9.04, and 8.74 [where log N(O) = 12 + log (O/H)]. The value 9.04 is the abundance which would be found in the Hyades given an identical O/Fe ratio to the Sun. The Hyades iron abundance assumed is that of Cayrel et al. (1985), while the solar oxygen abundance, log N(O) = 8.92, is from Lambert (1978) and Anders & Grevesse [1989; log N(O) = 8.93]. Using an equivalent assumption, with the iron abundance of the Ursa Major group taken from Boesgaard et al. (1988), the predicted oxygen abundance should lie within the range 8.74–9.34. The metallicities of the six field stars (Balachandran 1990a) are between the limits $-0.51 \leq$ [Fe/H] ≤ 0.24.

The code employed gives synthetic line profiles in either LTE or NLTE conditions. Using the theoretical profiles, we produced, via integration of the three individual lines, a grid of equivalent widths of the triplet as a whole in order to derive the O abundances by interpolating (in a few cases extrapolating slightly beyond the grid) the appropriate values for each star. Table 2 gives the oxygen abundances computed in LTE and NLTE for the measured equivalent widths in our observed spectra. For a subsample of 12 stars which show unblended lines, we also computed the oxygen abundances given by each line of the triplet. These stars are in the $T_{\rm eff}$ range 5900–7000 K. The abundances derived from the three lines in a given star are very similar, showing a typical rms dispersion of 0.12 dex. The abundances provided by the integrated triplet are in very good agreement with the mean value given by the three lines separately. A linear fit between these two values shows an rms deviation of 0.04 dex, indicating that for our stars the abundances derived in these two ways are essentially the same. We will show below that this is also true for the solar case. The use of the integrated triplet is, then, a useful tool for deriving oxygen abundances, and it is the only one that can be used in those stellar spectra with rotationally blended lines. The uncertainties assigned to the NLTE abundances in Table 2 were computed by taking the root of the squared uncertainties in the estimates of effective temperature (± 100 K which contributes ± 0.04 dex in the hottest models and ± 0.16 dex in the coolest) and surface gravity and microturbulence (with a maximum combined effect of ± 0.11 dex).

3.4.1. *The Solar Oxygen Abundance*

Since we wanted to carry out a differential study with respect to the Sun, we decided to calculate the solar oxygen abundance using the same procedure as for the stars. We measured the

equivalent width of the IR triplet of O I in the solar spectrum of Kurucz et al. (1984; which corresponds to the whole solar disk), using the integrated equivalent width in this case also. The value obtained, $W_\lambda(O) = 0.200 \pm 0.002$ Å can be contrasted with the values of 0.177 Å derived by summing the equivalent widths of the three lines measured individually by Kiselman (1991), or 0.192 Å obtained using the atlas of Moore et al. (1966). It is, however, in good agreement with the value $W_\lambda(O) = 0.202$ Å obtained by summing the equivalent widths given by Lambert (1978) and is very close to the value of $W_\lambda(O) = 0.212 \pm 0.002$ Å obtained by integrating over the triplet as a whole in the solar atlas of Delbouille, Roland, & Neven (1973). The three latter measurements come from solar disk center observations.

The solar oxygen abundance inferred directly from our NLTE analysis was log $N(O) = 9.16$. As in the stellar case, we made a test in order to compare this abundance and that given by the three lines measured separately on the Kurucz et al. (1984) atlas. The abundances provided by the three lines show a very good agreement, and the mean value is 9.16 ± 0.03. A similar example of internal consistency is found using the solar atlas of Delbouille et al. (1973) for this test (although the absolute abundances are 0.1 dex higher than before because this is a center disk spectrum which shows higher equivalent widths). The value obtained, 9.16, is 0.24 and 0.23 dex higher than the values derived by Lambert (1978) and by Anders & Grevesse (1989), respectively. Several parameters could contribute to this difference, and we can note, among others, the use of different model atmospheres, opacities, and our initial choice of van der Waals broadening parameter, C_6, which we will treat in more detail in the following paragraph. Lambert's LTE study used, as the key observation, measurements of the two lines of [O I] $\lambda\lambda$6300 and 6363, which are barely affected by NLTE effects, and which yield abundances with internal agreement better than 0.03 dex. On the other hand, Anders & Grevesse made use of a careful analysis of vibration rotation and pure rotation lines of molecules of CO and OH obtained from space observations.

As noted above, the value of C_6 which we employed in our synthesis code is 3 times smaller than the value which comes from a direct application of the Unsöld (1955) approximation (eq. [3]). Raising the value of C_6 yields higher values of the predicted equivalent width for a given abundance and model atmosphere, and so reduces the abundance required to match a given observed equivalent width. To quantify this, using Lambert's (1978) solar oxygen abundance as our bench mark, we computed a set of model profiles with different values of C_6, taken by multiplying the value given from equation (3) by 1, 3, and 6. The solar oxygen abundances inferred for this set of values were 9.12, 9.08, and 8.96, respectively. Thus to make our solar oxygen abundance compatible with those of Lambert (1978) or Anders & Grevesse (1989) we would need to adopt a value of C_6 which is $\sim$6 times that given by equation (3). The same result was obtained previously by Abia & Rebolo (1989) in their LTE analysis of the O I triplet, using a different synthesis code.

We have seen that we can explain the difference of 0.24 dex between our solar oxygen abundance and that from Lambert (1978) in terms of an increment in the broadening parameter C_6, but does this increment produce the same effect on the abundances derived for other models in the temperature range of interest in the present paper? To make an estimate of this we repeated the calculation just described for the Sun using a model atmosphere with $T_{\rm eff} = 7000$ K (referred to as 6 in Table 3) and taking an equivalent width $W_\lambda(O)$ of 0.6 Å, which we can see by inspecting Table 2 is representative of the observed values for stars with about this $T_{\rm eff}$. The differences found between the two sets of NLTE oxygen abundances (from solar and hotter models, respectively) show a high degree of uniformity within a value of 0.1 dex. This discrepancy of 0.1 dex may be simply due to the arbitrary choice of $W_\lambda(O)$, or it may be due to real differences between the stellar abundances and that of the Sun, or possibly a combination of both. So, we can consider that a change of a factor $\sim$6 in the C_6 value used in our analysis procedure corresponds directly with a change of scale of $\sim$0.2 dex in the oxygen abundance, which is valid for the effective temperature range in which we are interested. Obviously, this fact affects any attempt for evaluating the absolute oxygen abundance in our sample stars; however, the work presented below amounts to a differential analysis of the O abundances with respect to the Sun which is unaffected by these uncertainties. In Table 2 we give the value of [O/H] for each star, using an assumed solar oxygen abundance log $N(O) = 9.16$ derived as explained above. The use of this value for the solar oxygen abundance ensures the validity and consistency of the [O/H] values in our work.

3.4.2. *Comparison with Previous Measurements in the Hyades*

The oxygen abundances for two of the Hyades stars in our sample were previously measured by Tomkin & Lambert (1978) and later revised by Clegg, Lambert, & Tomkin (1981). These two stars are VB14 (45 Tauri) and VB37 (HD 27561). The revised value given by the latter authors for both stars is [O/H] = 0.15, which is higher than the values 0.02 ± 0.13 and -0.14 ± 0.15 obtained in our analysis for the two stars, respectively. The oxygen abundances for these stars were computed in LTE by Clegg et al. (1981) using the O I λ9266 line, but the solar oxygen abundance they used is log $N(O) = 8.92$ given by Lambert (1978), and obtained mainly from [O I] lines. The transition originating the λ9266 line is included in our model atom, and we were able to compute oxygen abundances for the two stars and the Sun using this line as indicator. We used two different values of log gf: 0.80 given by Wiese et al. (1966), and 0.71 provided by Biémont et al. (1991). The equivalent width measurements employed were taken from Tomkin & Lambert (1978) for VB14 (0.120 Å) and VB37 (0.86 Å), and from Lambert (1978) for the solar case (0.031 Å). The effective temperature adopted for VB37 (6815 K) differs slightly from Tomkin & Lambert's (1978) estimate (6750 K), and log $g = 4.2$ was used in our grid of models in contrast with the value 4.0 employed by these authors. Although the excitation potential of the λ9266 line is high (10.74 eV) the differences between the abundances computed in LTE and NLTE are small: less than 0.1 dex for the solar case and $\sim$0.1 dex for 7000 K. The [O/H] values obtained in LTE for these two stars via the λ9266 line, and using the solar oxygen abundance computed following the same procedure, are 0.12 and -0.10 for VB14 and VB37, respectively. This result is independent of the log gf value adopted. The corresponding NLTE values are [O/H] = 0.08 and [O/H] = -0.13. A decrease of 0.2 dex in log g produces a decrease of 0.1 dex in these abundances. We see that there is a clear agreement between these NLTE results for the λ9266 line and our [O/H] values computed from the O I IR triplet. The difference compared with the [O/H] values in Clegg et al. (1981) seems to come from their use of a solar abundance, which although correct in absolute terms, was derived from

different lines from those employed in the analysis for the stars. An additional indication of this can be seen by inspecting Table 6 of Clegg et al. (1981) which lists [O/H] values derived from several lines of O I and [O I] for 20 F and G main-sequence stars. In four of the five cases in which there are abundances derived from both the [O I] λ6300 line and the O I $\lambda\lambda$9260, 9262, and 9266 lines, the abundance provided by the first line is smaller than that obtained from the other three lines with a mean difference of 0.15 ± 0.12 for the five stars (with effective temperatures in the range 5800–6200 K).

4. RESULTS AND DISCUSSION

The results of our NLTE analysis of the infrared triplet are presented in Figure 3, where we plot [O/H] against $T_{\rm eff}$. We also show the lithium abundances for the same stars, taking the Hyades values from Boesgaard & Tripicco (1986a), Boesgaard (1987b), and Boesgaard & Budge (1988), those for the Ursa Major group from Boesgaard et al. (1988), and for the six slightly evolved field stars from Balachandran (1990a).

A notable feature of Figure 3 is that, in contrast to lithium, oxygen shows no major abundance "gap" in the effective temperature range considered. The average value of the abundance for all the stars observed is [O/H] = −0.05 with a standard deviation of 0.17 dex, which is compatible with the uncertainties in the individual estimates. Taking each group separately, the abundances are -0.06 ± 0.15 for the Hyades, -0.06 ± 0.20 for the Ursa Major group, and $+0.02 \pm 0.18$ for the field stars. To examine the dependence of [O/H] on $T_{\rm eff}$ we can divide the figure into three different zones (neglecting the hottest star in the sample, which we will treat in detail below), viz., zone A, with $T_{\rm eff}$ between 7150 and 6830 K, zone B between 6830 and 6450 K, and zone C between 6450 and 5800 K. There appears to be a slight dip in the abundance of oxygen in zone B, notably in the stars of the Ursa Major group, where the mean abundances for the three zones are

A	B	C
$+0.21 \pm 0.19$	-0.23 ± 0.06	-0.09 ± 0.13 .
4 stars	5 stars	9 stars

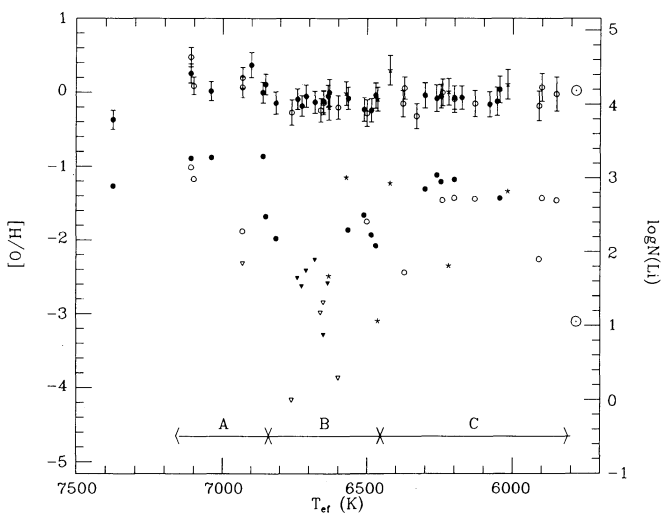

FIG. 3.—Oxygen and lithium abundances for the stars in our sample vs. $T_{\rm eff}$. Symbols as in Fig. 2. Note the clear absence of an oxygen gap in the region in which the Li gap is present. Stars in the zone B might be indicating a very small oxygen dip, <0.1 dex, with respect to the stars located in region C.

The error quoted for each group is the standard deviation with respect to the mean value of the group. The corresponding values for the Hyades are

A	B	C
$+0.15 \pm 0.16$	-0.11 ± 0.08	-0.07 ± 0.06 .
5 stars	12 stars	8 stars

For the Hyades the scatter in [O/H] for the cool group, C, is less than for the Ursa Major group, but the difference between the abundances in groups B and C is also less. Combining the two clusters produces

A	B	C
$+0.18 \pm 0.16$	-0.15 ± 0.09	-0.08 ± 0.10 .
9 stars	17 stars	17 stars

We see that the mean abundance in group B is some 2 σ lower than that of group A, and $\sim 1\ \sigma$ lower than for group C. The six F-type field stars, slightly evolved from the main sequence according to Balachandran (1990a) also appear to follow a similar pattern to the stars in the clusters, with the exception of HR5363 ($T_{\rm eff} = 6240$ K) which shows a higher abundance, similar to those of region A. This is a star with an absolute visual magnitude of $M_V = 2.4$ which, according to the evolutionary tracks of VandenBerg (1985), has a mass of 1.5 $M_\odot$ and spent its life on the main sequence at the $T_{\rm eff}$ zone A, a fact which is compatible with its oxygen abundance.

The dispersions for samples B and C are equal, and less than for sample A, where a smaller number of stars was measured. An overall conclusion from these measurements is that there is no major change in oxygen abundance across the temperature range sampled although there is a possible, not statistically definitive, small dip in the abundance for group B. We must also draw attention here to the notable absence of oxygen in the hottest star of the sample VB38 ($T_{\rm eff} = 7375$ K).

Let us first discuss the anomalous result for this latter object. This is related to the object being a chemically peculiar star, of type Am-Fm. VB38 figures as a well-known Am star in the *General Catalog of Ap and Am Stars* recently published by Renson, Gerbaldi, & Catalano (1991). The Am stars are found with effective temperatures in the range 7000–10,000 K and are characterized by a set of chemical anomalies compared with "normal" stars. To summarize, we can say that they are found to be deficient in Ca and Sc by a factor between 5 and 10, while the iron group elements are overabundant by between 2 and 3, and certain rare earths also show overabundances by factors of order 10. Their Li abundances are either the standard cosmic value found in very young stars or underabundant, but they are never overabundant (Burkhart & Coupry 1989; Cayrel, Burkhart, & van't Veer 1991). As far as C, N, and O are concerned, the works of Roby & Lambert (1990) and of van't Veer-Menneret et al. (1989), the latter devoted exclusively to oxygen, shows that these elements are normally deficient in Am stars, with a deficiency which is largest at the lowest temperatures and which decreases with increasing effective temperature, becoming virtually negligible in the Am stars with highest $T_{\rm eff}$. Boesgaard & Tripicco (1986a) found log N(Li) = 2.89, and [Fe/H] = +0.29 for VB38; this iron abundance is 0.13 dex higher than the mean of 0.16 ± 0.09 for their cluster sample. These Li and Fe observations are therefore compatible with the explanation that the underabundance of oxygen we find is due to VB38 being a star of type Am-Fm.

Proceeding toward lower $T_{\rm eff}$, we next consider the oxygen abundances of group A. This group shows the highest scatter,

as can be seen in Figure 3. This scatter could simply be due, as noted above, to the smaller size of this sample compared with samples B and C. If the suggestion of Michaud (1988) that the observed oxygen abundance could be affected by microscopic diffusion were in fact correct, the increase in the outward radiative pressure in the hotter stars would tend to accelerate the O atoms toward the surface, producing a tendency to higher observed abundances at higher $T_{\rm eff}$, rather than a uniform value. Our results, showing only a slightly increased dispersion in group A compatible with the small sample, do not point clearly in the direction of such a trend, but could not be used as evidence against the suggestion. In fact the mean abundance of group A is some 0.3 dex higher than the mean for the cooler stars, just on the border of statistical significance, taking the observed dispersions into account. We must leave this as an open question for yet more comprehensive observations and theoretical calculations.

For the stars in temperature range B, the data show a slightly lower abundance, by 0.07 dex, than the stars in the cooler range C. If this small dip were in fact real, that is, if there were a real underabundance of oxygen in stars of zone B compared with both cooler and hotter objects, this phenomenon should be due to microscopic diffusion of the oxygen atoms below the base of the convection zone. There is, in principle, no other known mechanism able to produce this kind of depletion in the abundance of a chemical element which is not destroyed by nuclear burning in the stellar interior. The B range coincides broadly with the range of spectral types where the lithium gap has been detected for the clusters. For those who wish to invoke the diffusion hypothesis for producing the Li gap, our present oxygen measurements place a clear observational restriction on the working of this mechanism. It must be capable of reducing the Li abundance by up to two orders of magnitude, while leaving the oxygen unaffected, or almost unaffected, with reductions lower than 0.1 dex. These restrictions apply directly, with these numbers, only, of course, to the two clusters observed which have ages less than 10^9 years. Detailed computations for oxygen diffusion would be required to make a direct comparison with the observations.

On the other hand, we can make a tentative alternative suggestion with respect to both the Li gap and the possible small oxygen dip. It is clear that the presence of turbulence will affect the simplest schemes of microscopic diffusion in which hydrostatic equilibrium is disturbed by an imbalance between gravitational and radiative accelerations. It does seem to be necessary to invoke the modification of diffusion by turbulent mixing to explain certain observations, for example, the abundance of Li in subgiants of the open cluster M67, which should have been in the Li gap while on the main sequence, but do not show the abundances expected if the Li which had diffused below the surface during this phase were now released to the surface in the subgiant phase (Balachandran 1990b). In attempts to include the effects of turbulence, this has been done directly by introducing an additional turbulent diffusion coefficient in the transport equation (Charbonneau & Michaud 1990, 1991; Proffitt & Michaud 1991; Charbonnel et al. 1992). Although this does indeed take turbulence into account, any effects of the interaction between turbulence and microscopic diffusion have been neglected. We can qualitatively suggest a possible scenario to explain the Li and O observations, in which this interaction would play a role. Given a degree of turbulence within the star, associated with rotation, rotational braking, or the presence of internal gravity waves, the effect of the combination of microscopic diffusion and turbulence would be, in the $T_{\rm eff}$ range of the Li gap, to pull the Li atoms down to the level where they are destroyed by nuclear burning. On the other hand, the turbulent mixing would attenuate the effect of the microscopic diffusion on the O atoms. Since these are not destroyed, mixing with the interior will not notably affect the surface abundance. If the slight dip in the O abundance we appear to detect in range B were real, this could be due to the residual effect of the microscopic diffusion, as would the slightly raised abundance in range A. With observational effects of such small amplitude, however, more quantitative and testable conclusions must await more observations.

Finally we look at the mean abundance of oxygen in range C. These stars show a rather uniform oxygen abundance, very comparable with the solar value, and there are no theoretical reasons to expect effects of transport processes on their oxygen atoms. The measurements in this group of stars can be used to examine the evolution of the oxygen abundance against metallicity for solar neighborhood stars. Cluster stars have the advantage over field stars of giving well-determined values both for metallicity and age. We have incorporated the data in a global plot of [O/H] versus [Fe/H] for solar-type disk stars. This is shown in Figure 4, where the data for field stars have been taken from Nissen & Edvardsson (1992). They observed and analyzed the forbidden line [O I] λ6300 in a sample of 23 F and G stars covering a metallicity range from +0.3 to −0.8. The effective temperature of the stars studied by these authors comprises the range 5730–6705, with all but two of the stars with $T_{\rm eff}$ located in zone C. We took the mean iron abundances for the Hyades from Cayrel et al. (1985), and from Boesgaard et al. (1988) for the Ursa Major group. Because in both cases the iron abundances were computed using Fe I lines, we also took the [Fe/H] values for the field stars from Fe I determinations by Edvardsson et al. (1992) as given in Nissen & Edvardsson (1992). As can be seen in Figure 4, the two points corresponding to the clusters, which represent data from eight stars of the Hyades and nine stars from the Ursa Major group, lie well

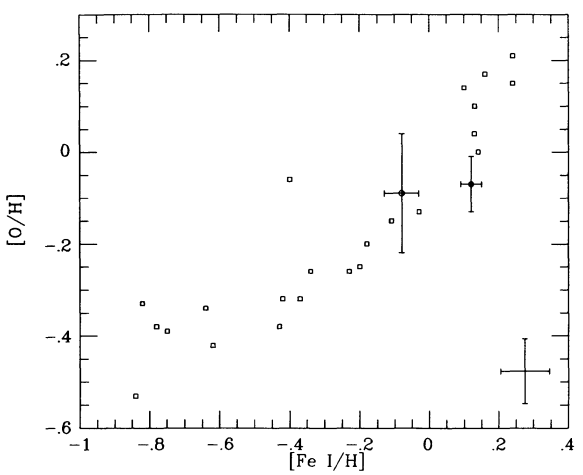

FIG. 4.—[O/H] vs. [Fe/H] for a group of solar-type stars of the nearby Galactic disk, from Nissen & Edvardsson (1992), derived using the [O I] λ6300 and Fe I lines. We have added the two points we obtain from eight stars in the Hyades (*filled circle*) and nine stars in the Ursa Major group (*open circle*) from our O I IR triplet abundance analysis in the $T_{\rm eff}$ range 5800–6450 K, together with their error bars which represent the standard deviation with respect to the mean. Typical error bars for a single field star determination are shown at the right bottom corner.

within the strip covered by the field stars, showing a monotonic increase of the oxygen abundance with metallicity. We note, however, the strong scatter and apparent change of slope in this trend for stars with [Fe/H] > 0.

Nissen & Edvardsson (1992) have studied the evolution of [O/H] against age for their sample of solar-type field stars (their Fig. 7). The ages for their field stars were derived by comparing the position in the $T_{\rm eff}$–M_V diagram with isochrones computed by VandenBerg (1985). They find a trend to higher [O/H] values when decreasing the stellar age, with a large scatter at a given age. In Figure 5 we have reproduced Figure 7 of Nissen & Edvardsson including our data for the Hyades and Ursa Major group. The ages for the two clusters studied are much more accurate than for the disk stars, allowing us to add two very precise points in the [O/H] versus age diagram. Adding the new data obtained for the clusters indicates a flatter relation than that previously inferred for field stars only, showing an asymptotic trend to [O/H] ratios close to the solar value with decreasing age. There is in fact a clear discrepancy between the relation which could be extrapolated using the field stars alone and that which emerges when cluster data are included. A similar discrepancy can be found when plotting [Fe/H] versus age using data for several open clusters, with ages in the range 5×10^7–5×10^9 yr, taken from García López, Rebolo, & Beckman (1988), Boesgaard (1989), and Friel & Boesgaard (1992). The group of field stars showing a deviation of the tendency in Figure 5 is also the same as that which shows enhanced scatter in Figure 4. More oxygen abundance measurements in metal-rich field dwarf stars are necessary to study in more detail the extent of this controversy. On the other hand, we suggest that the best way to study the evolution of the oxygen abundance in the Galactic disk during the last 5×10^9 yr is by measuring the oxygen abundance in solar-type stars belonging to open clusters with different ages, in which both age and O abundance can be measured with a high level of accuracy.

5. CONCLUSIONS

We have observed the O I infrared triplet in a sample comprising 50 F-type stars, 25 from the Hyades, 18 from the Ursa Major group, and six field stars. We have derived their oxygen abundances, and that of the Sun, using an NLTE analysis. From a self-consistent differential abundance analysis with respect to the Sun we derived the following main conclusions:

1. There is relatively little departure from uniformity in the O abudances for all the stars in the sample, for a range of $T_{\rm eff}$ between 5800 and 7400 K.

2. The data may indicate a very small dip in the O abundance (<0.1 dex) for the stars in the $T_{\rm eff}$ range of the "lithium gap" and a small rise (~0.3 dex) at higher temperatures. Microscopic diffusion appears to be the only known mechanism able to produce an oxygen dip. The rather tight limit to the oxygen deficiency in the Li gap acts as a serious constraint on the microscopic diffusion hypothesis: the mechanism must be capable of accounting for a depletion up to two orders of magnitude in Li without a notable corresponding decrease in O. The presence of turbulent mixing might modify the microscopic diffusion process in such a way as to explain both Li and O observations.

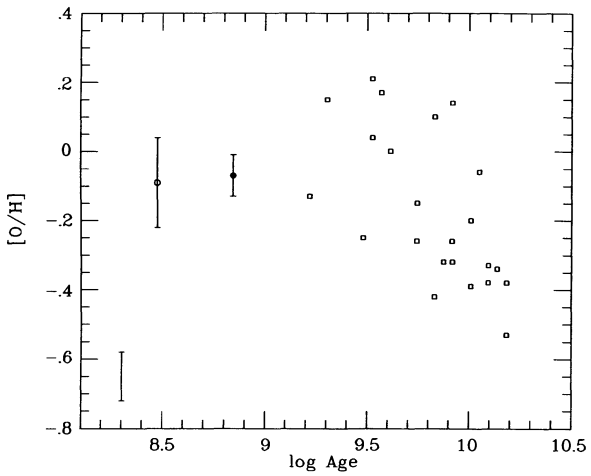

FIG. 5.—[O/H] vs. age for the same stars than in Fig. 4. A typical error bar for [O/H] in field stars is shown at the left bottom corner.

3. The hottest star in our sample, VB38 in the Hyades, shows an appreciably lower oxygen abundance than the remaining sample stars. This is consistent with the object being an Am-Fm star.

4. The measured ratios of [O/H] for the Hyades and the Ursa Major group, which represent data for eight and nine stars, respectively, with effective temperatures in the range 5800–6450 K, fit well the general trend of [O/H] versus [Fe/H] observed for solar-type stars in the Galactic disk between [Fe/H] = +0.3 and −0.8. There is, however, a large dispersion for stars with [Fe/H] > 0. The [O/H] values for the clusters (which have a more accurate age determination) imply an evolution of [O/H] with age which is flatter with decreasing age than that derived using only disk stars.

The authors are grateful to P. E. Nissen for the communication of his oxygen results prior to publication. The useful comments from the anonymous referee have contributed to clarifying several points in the article. This work was partially supported by the Spanish DGICYT under project PB90-0548.

Note added in manuscript.—Recently de Freitas Pacheco [(1993), ApJ, 403, 673] has shown that the oxygen abundance in type I planetary nebulae, whose progenitors are younger than 1–2 Gyr, seems to be 0.2 dex lower than the solar value. This is also in agreement with the oxygen abundances derived by other authors in H II regions, B-type stars of young associations, and in F-K supergiants with metallicities comparable to the Hyades value. Our results for the Hyades and the Ursa Major group show a mean oxygen abundance [O/H] ~ −0.1 for solar-type stars (group C) in both clusters, thus providing additional support for the idea that the stars formed recently have oxygen abundances compatible with the ISM value and lower than the solar abundance. The possible discrepancy between these results and the oxygen abundances in the younger F and G disk stars of Nissen & Edvardsson's (1992) sample should be studied in detail in order to delineate the oxygen evolution in the Galactic disk precisely.

REFERENCES

Abia, C., & Rebolo, R. 1989, ApJ, 347, 186
Anders, E., & Grevesse, N. 1989, Geochim. Cosmochim. Acta, 53, 197
Auer, L. H., & Heasley, J. N. 1976, ApJ, 205, 165
Balachandran, S. 1990a, ApJ, 354, 310
———. 1990b, ASP Conf. Series, 9, 357
———. 1991, in IAU Symp. 145. Evolution of Stars: the Photospheric Abundance Connection (Poster Papers), ed. G. Michaud, A. Tutukov, & M. Bergevin (Montreal: Univ. Montreal), 13
Baschek, B., Scholz, M., & Sedlmayr, E. 1977, A&A, 55, 375
Beckman, J. E., & Rebolo, R. 1988, in IAU Symp. 132, The Impact of Very High S/N Spectroscopy on Stellar Physics, ed. G. Cayrel de Strobel & M. Spite (Dordrecht: Kluwer), 473
Bessell, M. S., Sutherland, R. S., & Ruan, K. 1991, ApJ, 383, L71
Biémont, E., Hibbert, A., Godefroid, M., Vaeck, N., & Fawcett, N. 1991, ApJ, 375, 818
Boesgaard, A. M. 1987a, PASP, 99, 1067
———. 1987b, ApJ, 321, 967
———. 1989, ApJ, 336, 798
Boesgaard, A. M., & Budge, K. G. 1988, ApJ, 332, 410
Boesgaard, A. M., Budge, K. G., & Burck, E. E. 1988, ApJ, 325, 749
Boesgaard, A. M., & Tripicco, M. J. 1986a, ApJ, 302, L49
———. 1986b, ApJ, 303, 724
———. 1987, ApJ, 313, 389
Burkhart, C., & Coupry, M. F. 1989, A&A, 220, 197
Butler, K., & Giddings, J. R. 1985, Newsletter on Analysis of Astronomical Spectra, ed. A. E. Lynas-Gray (London)
Cayrel, R., Burkhart, C., & van't Veer, C. 1991, in IAU Symp. 145, Evolution of Stars: The Photospheric Abundance Connection, ed. G. Michaud & A. Tutukov (Dordrecht: Kluwer), 99
Cayrel, R., Cayrel de Strobel, G., & Campbell, B. 1985, A&A, 146, 249
Charbonneau, P., & Michaud, G. 1988, ApJ, 334, 746
———. 1990, ApJ, 352, 681
———. 1991, ApJ, 370, 693
Charbonnel, C., Vauclair, S., & Zahn, J.-P. 1992, A&A, 255, 191
Clegg, R. E. S., Lambert, D. L., & Tomkin, J. 1981, ApJ, 250, 262
Cowan, R. D. 1981, The Theory of Atomic Structure & Spectra (Berkeley: Univ. California Press)
Crawford, D. L., & Perry, C. L. 1966, AJ, 71, 206
de Freitas Pacheco, J. A. 1993, ApJ, 403, 673
Delbouille, L., Roland, G., & Neven, L. 1973, Atlas Photometrique du Spectre Solaire
Edvardsson, B., Andersen, J., Gustafsson, B., Lambert, D. L., Nissen, P. E., & Tomkin, J. 1992, in preparation
Eriksson, K., & Toft, S. C. 1979, A&A, 71, 178
Faraggiana, R., Gerbaldi, M., van't Veer, C., & Floquet, M. 1988, A&A, 201, 259
Friel, E. D., & Boesgaard, A. M. 1992, ApJ, 387, 170
García López, R. J., Rebolo, R., & Beckman, J. E. 1988, PASP, 100, 1489
García López, R. J., & Spruit, H. C. 1991, ApJ, 377, 268
Giddings, J. R. 1981, Ph.D. thesis, Univ. London
Gray, D. F. 1976, The Observation and Analysis of Stellar Photospheres (New York: John Wiley)
Hauck, B., & Mermilliod, M. 1980, A&AS, 40, 1
Hibbert, A. 1975, Comput. Phys. Comm., 9, 141
Hobbs, L. M., & Pilachowski, C. A. 1986, ApJ, 309, L17
———. 1988, ApJ, 334, 734
Hoffleit, D., & Jaschek, C. 1982, The Bright Star Catalogue
Hofsaess, D. 1979, Atomic Data Nucl. Data Tables, 24, 285
Kiselman, D. 1991, A&A, 245, L9
Kraft, R. P. 1965, 142, 681
Kurucz, R. L. 1979, ApJS, 40, 1
Kurucz, R. L., Furenlid, I., Brault, J., & Testerman, L. 1984, Solar Flux Atlas from 296 to 1300 nm, NOAO Atlas No. 1
Lambert, D. L. 1978, ApJS, 65, 255
Lambert, D. L., Heath, J. E., & Edvardsson, B. 1991, MNRAS, 253, 610
Mermilliod, J.-C. 1976, A&AS, 24, 159
Michaud, G. 1986, ApJ, 302, 650
———. 1988, in IAU Colloq. 108, Atmospheric Diagnostic of Stellar Evolution: Chemical Peculiarities, Mass Loss, and Explosion, ed. K. Nomoto (New York: Springer), 3
Moore, C. E., Minnaert, M. G. J., & Houtgast, J. 1966, NBS Monograph, No. 61
Nissen, P. E. 1981, A&A, 97, 145
Nissen, P. E., & Edvardsson, B. 1992, A&A, 261, 255
Pinsonneault, M. H., Kawaler, S. D., & Demarque, P. 1990, ApJS, 74, 501
Proffitt, C. R., & Michaud, G. 1991, ApJ, 380, 238
Renson, P., Gerbaldi, M., & Catalano, F. A. 1991, A&AS, 89, 429
Roby, S. W., & Lambert, D. L. 1990, ApJS, 73, 67
Saxner, M., & Hammarbäck, G. 1985, A&A, 151, 372
Schramm, D. N., Steigman, G., & Dearborn, D. S. P. 1990, ApJ, 359, L55
Seaton, M. J. 1962, in Atomic & Molecular Processes, ed. M. Bates (New York: Academic), chap. 11
Sedlmayr, E. 1974, A&A, 31, 23
Sneden, C., Lambert, D. L., & Whitaker, R. W. 1979, ApJ, 234, 964
Tomkin, J., & Lambert, D. L. 1978, ApJ, 223, 937
Unsöld, A. 1955, Physik der Sternatmosphären (Berlin: Springer)
van Regemorter, H. 1962, ApJ, 136, 906
VandenBerg, D. C. 1985, ApJS, 58, 711
van't Veer-Menneret, C., Faraggiana, R., Gerbaldi, M., Castelli, F., Burkhart, C., & Floquet, M. 1989, A&A, 224, 171
Vauclair, S. 1988, ApJ, 335, 971
Wiese, W. L., Smith, M. W., & Glennon, B. M. 1966, Atomic Transition Probabilities, Vol. 1 (NSRDS-NBS4; Washington: GPO)